

Design and test of automatic detection platform for soil fragmentation rate in rotary tillage

Xinwu Du^{1,2}, Xulong Yang¹, Jing Pang¹, Jiangtao Ji^{1,2*}

(1. College of Agricultural Equipment Engineering, Henan University of Science and Technology, Luoyang 471003, Henan, China;
2. Advanced Manufacturing of Mechanical Equipment Henan Collaborative Innovation Center, Luoyang 471003, Henan, China)

Abstract: As an important index of soil crushing performance of rotary tiller, the soil fragmentation rate is still limited to manual measurement. In this study, an automatic detection platform for soil fragmentation rate was designed, which integrated soil intake, screening, weighing and calculation of soil fragmentation rate. This platform can solve the problem that the index of the soil fragmentation rate cannot be detected quickly and effectively after rotary tillage, which leads to difficulty in field quality evaluation. The platform was mainly composed of a shovel soil module, conveying module, screening module, weighing module and automatic control system, which could realize single-line and multi-point automatic soil fragmentation rate detection. Based on the homogeneous dry slope model, the tilting angles of soil intake and soil feeding after rotary tillage on the platform were determined to be 30.10° and 26.67°, respectively. According to the principle of flow conservation, a rotary circulation screening module was designed to obtain soil particle size grading. A method based on the principle of multi-line and multi-point measurement was developed to detect soil fragmentation rate. The influence of screening speed on screening effect was analyzed, and the reasonable value of screening speed was determined to be 0.5 m/s. A field performance test was carried out in October 2019 to verify the detection performance of the platform. The results showed that, compared with the manual test method, the maximum test error was no more than 11%, the minimum test error was less than 4%, the maximum single test time was no more than 2 min, and the total test time of each test area was no more than 30 min. The efficiency of single-point detection was significantly better than the manual detection, which indicated that the design in this study met the requirements of rapid detection of soil fragmentation rate, and provided a new idea for the automatic detection of quality of rotary tillage.

Keywords: rotary tillage, soil fragmentation rate, automatic detection, design, test

DOI: 10.25165/j.ijabe.20201305.5678

Citation: Du X W, Yang X L, Pang J, Ji J T. Design and test of automatic detection platform for soil fragmentation rate in rotary tillage. Int J Agric & Biol Eng, 2020; 13(5): 40–49.

1 Introduction

The quality of rotary tillage includes operating depth, surface flatness, vegetation coverage and soil fragmentation. In these technical indexes, the soil fragmentation rate represents the probability distribution of soil mass geometry after tillage and is one of the important parameters to measure the performance of rotary tiller. Therefore, the rapid and accurate detection of soil fragmentation rate after tillage has important guiding significance to the performance rating of agricultural production and rotary tiller. According to technical standards for agricultural machinery NY/T 499-2013 “Quality of rotary tiller operation” in China, the detection methods of soil fragmentation rate mainly including a visual method and manual screening method. The visual method relies on observation of soil fragmentation after tillage and evaluates the effect of rotary tillage according to experience. The manual

screening method is based on the five-point measurement principle. All cultivated soil samples within a certain area are screened, classified and weighed manually, and the percentage of the soil mass with the longest side less than or equal to 40 mm in the total soil sample mass is taken as the soil fragmentation rate^[1-3]. The former completely depends on human experience estimation, although it can quickly guide agricultural production, it cannot quantitatively show the effect of soil fragmentation, and there is a huge error; The latter usually requires the cooperation of several people, which is not only labor-intensive and takes a long time to measure but also causes secondary damage to the cultivated soil. Therefore, it is very necessary to design automatic and rapid test equipment for soil fragmentation rate after tillage.

In recent years, there were little researches on soil fragmentation rate in the world, but it was very common to take soil fragmentation rate as the detection index^[4-9]. Bayat H et al.^[10] established relationship between penetration resistance, bulk density and water content by collecting Iranian soil samples based on the feedforward neural networks, and believed that it is more convenient to estimate soil conditions by measuring penetration resistance and moisture content than by measuring other parameters. Goodin C et al.^[11] used the smoothed particle hydrodynamics (SPH) method to simulate cone penetrometer tests in cohesive soil, and analyzed the relationship between soil resistance and soil density. Celik A et al.^[12] studied the soil disturbance caused by different types of rotary cultivators and measured the relationship between the shape of plough blade and soil disturbance, cone index and bulk

Received date: 2020-01-14 **Accept date:** 2020-07-13

Biographies: **Xinwu Du**, PhD, Associate Professor, research interest: agricultural mechanization technology, Email: du_xinwu@sina.com; **Xulong Yang**, Master candidate, research interest: design and manufacture of agricultural machinery, Email: hkyangxulong@163.com; **Jing Pang**, PhD, research interest: agricultural machinery performance testing technology, Email: 529565328@qq.com.

***Corresponding author:** **Jiangtao Ji**, PhD, Professor, research interest: agricultural automatic detection technology. Henan University of Science and Technology, Luoyang 471003, Henan, China. Tel: +86-379-64877817, Email: jjt0907@163.com.

density. In China, Wang et al.^[13] optimized the parameters of the leveling parts of the combined tillage machine by adopting the manual screening method and taking the soil fragmentation rate as the index according to China's technical standard JB/T10295-2001 "Combined implement for subsoiler and cultivating". Qin et al.^[14] used GB/T5668-2008 "Rotary tiller" to manually test the soil fragmentation rate index of the plowing and rotary tillage combined machine. The manual screening method was widely used in quality inspection of rotary tillage, but there was no other effective method to replace manual measurement^[15-19]. Xia et al.^[20] used image processing technology to explore the soil fragmentation rate of the micro-tiller, and calculated the soil fragmentation rate approximately by the ratio of the soil area to the sampling area meeting the size requirements. Although this method avoids the secondary crushing of soil, the maximum error was more than 14% compared with the manual screening method, which was mainly due to the inconsistencies of soil fragmentation rates in different soil layers. Liu et al.^[21] studied the heterogeneity of soil particle size distribution and the spatial variability of soil particle size distribution by using multifractal, geostatistical, and joint multifractal methods. The results showed that the heterogeneity of soil particle size distribution in different soil layers had certain variability. Therefore, the determination of soil fragmentation rate cannot be limited to soil surface detection.

The above research work has done much meaningful work for studying soil fragmentation rate measurement. However, these methods were mainly based on finite element simulation, or by measuring other soil parameters to indirectly calculate the soil fragmentation rate. There are errors between these measurement methods and the real situation, so it is necessary to directly measure the soil fragmentation rate. In this work, an automatic detecting platform for soil fragmentation rate after rotary tillage was designed. The platform could automatically complete the process of soil grasping, screening, weighing and calculating soil fragmentation rate. The advantage of this platform was that multi-line and multi-point measurements were used instead of five-point measurements to quickly detect the soil fragmentation rate. This would provide a direct and efficient method to detect the operation effect of the rotary tiller.

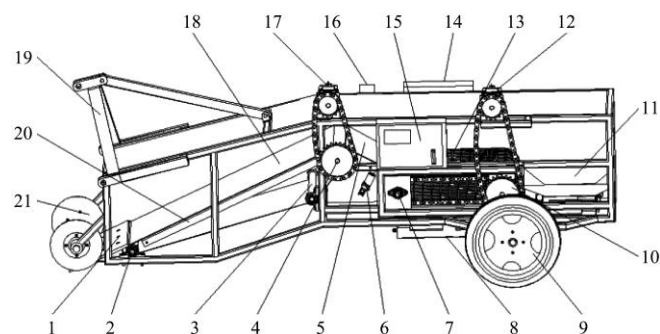
2 Design scheme and principle of detection platform

2.1 Overall structure design

The automatic detection platform for soil fragmentation rate in rotary tillage operation, referred to as the ADP-SFR, was shown in Figure 1. According to the function, the automatic detection platform could be divided into a shovel module, conveying module, screening module, weighing module and control system module. The whole machine relied on the tractor to provide traction power and adopt a 48V DC power supply to supply power to the platform during operation.

In the front end of the whole machine, the interface connecting with the three-point suspension mechanism of the tractor was designed, and the wheels were arranged at the rear end for walking. Below the interface, a shovel module was arranged, including a shovel and a disc cutter on either side of the interface. The conveyor module at the end of the shovel was carried on by chain drive, which was mainly composed of a conveyor belt, driving drum, turning drum, supporting plate and conveyor motor. At the end of the conveying module, the movable bridge was composed of a movable plate and an electric push rod, and it adopts the stretching of the electric push rod to realize the opening and closing

function of the movable bridge. The screening module at the end of the bridge was driven by a chain, which was mainly composed of the support frame, screening motor, screening mesh, driving shaft and driven shaft. The support frame was fixed on the rack, and the main and driven shafts were fixed by bearings at both ends respectively, and the mesh of the tooth chain drives the screening mesh to move. A weighing module was arranged under a screening mesh, including a weighing box for broken soil and a weighing box for large clods to collect broken soil and large clods respectively. Weighing sensors were arranged on both sides of the two boxes, one end of which was fixedly connected with the box body and the other end was fixedly connected with the frame, to measure the weight of the box body. A dynamic inclination sensor was installed on the frame to dynamically measure the change of its biaxial inclination, which could capture the attitude information of the ADP-SFR in real-time, and then compensate for the weight error caused by the change of inclination. The ADP-SFR could quickly complete the processes such as soil sampling, soil screening, weighing and calculation of soil fragmentation rate, and realize the detection of soil fragmentation rate at multiple measurement points with a single stroke. The main technical parameters were shown in Table 1.



1. Shovel 2. Turning drum 3. Tensioning shaft 4. Driving drum 5. Movable plate 6. Electric push rod 7. Driven shaft 8. Weighing box for broken soil 9. Wheels 10. Driving shaft 11. Weighing box for large clods 12. Screening motor 13. Screening mesh 14. Power supply 15. Control cabinet 16. Dynamic inclination sensor 17. Conveyor motor 18. Conveyor belt 19. Interface 20. supporting plate 21. Disc cutter

Figure 1 Schematic diagram of the whole machine

Table 1 Structural parameters of ADP-SFR

Parameters	Parameter value
Overall dimensions (Length×width×height) /mm×mm×mm	3000×1400×1042
Machine weight/kg	950
Traction power/kW	≥51.4
Supply voltage/V	48
Speed of operation/km h ⁻¹	0.5
Width of operation/mm	500
Depth of operation/mm	100-200
Method of limiting depth	Limit depth wheel
Type of screening	Diamond mesh
Mesh diameter of the screening/mm	40
Center distance of screening/mm	600
Volume of weighing box for broken soil/L	50
Volume of weighing box for large clods/L	25

2.2 Detection principle

After rotary tillage, the determination of the soil fragmentation rate in the field followed the multi-line and multi-point measurement method, and the detection strategy was shown in Figure 2. Compared with the five-point method, the multi-line

and multi-point method covers a wider range of measuring points and could reflect the field conditions more truly. The detection method had three lines, and several measuring points were set under each trip, and the total amount of soil samples was obtained according to NY/T499-2013 "quality of rotary tiller operation". The principle of soil fragmentation detection was as follows:

$$E_{ij} = \frac{m_a}{m_b} \times 100 \quad (1)$$

where, E_{ij} is the soil fragmentation rate at the measuring point j in stroke i , %; m_a is the mass of soil mass with the longest side less than 40 mm in the soil sample, kg; m_b is the total mass of all soil samples at the measuring point, kg.

$$E = \frac{\sum_{i=1}^m \sum_{j=1}^n E_{ij}}{mn} \times 100 \quad (2)$$

where, E is the average soil fragmentation rate, %; m is the number of lines, which was 3; n is the number of measuring points.

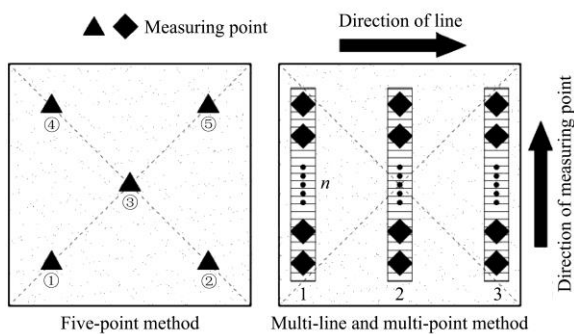


Figure 2 Detection method for soil fragmentation rate

When working, the ADP-SFR was suspended behind the tractor, which was driven forward by the tractor and the shovel was controlled to rise or fall by hydraulic adjustment of the three-point suspension mechanism on the tractor. At this point, the conveyor module enters the working state, the movable bridge was in the normally open state, and the soil was scooped up, transported to the height by conveyor belt and returned directly to the field. When the platform runs smoothly, the active bridge was closed and the screening module was started, which allows the soil to reach the mesh through the movable bridge. Then the soil was sifted into two separate boxes. When the total mass of soil in the weighing module reaches a pre-set threshold, the movable bridge was opened to block soil transport. According to the attitude information of the whole machine and the soil quality information in the weighing module, the control system module uses Equation (1) to calculate the soil fragmentation rate at the measuring point. Then unload the soil in the weighing module, and continue to measure the soil fragmentation rate of other measuring points on the line according to the above process. After the multi-line measurement, calculate the soil fragmentation rate of the whole measurement process according to Equation (2).

3 Key component design

3.1 Inclination of shoveling and conveying soil

In the process of shoveling and transporting soil, a slope was formed between the soil sample and the shovel or conveyor belt, also known as a soil slope. If the shear stress caused by the weight of the soil was greater than the shear strength of the soil, shear failure would occur, which causes a part of the soil with respect to another part of the soil sliding phenomenon was called landslide^[22-24]. Landslides occur while shoveling or transporting

soil would not only lead to the mixing of soil samples but also may lead to sampling discontinuity, which would affect the measurement results. Therefore, it was necessary to analyze the stability of soil slope according to the slope angle of the shovel or conveyor belt. Slope stability analysis methods mainly include the limit equilibrium method, limit analysis method and finite element method. In this work, the most common limit equilibrium method in engineering was used for analysis. Since the dryland soil after rotary tillage was mainly gravel soil with loose and granular characteristics, which could be equivalent to cohesionless soil, that is, the cohesion is equal to 0, so the dryland slope was simplified as a cohesionless homogeneous dry slope model.

Set the weight of a small soil element on the slope as W , as shown in Figure 3. The soil element produces a sliding force ($T=W\sin\alpha$) on the slope, which causes the soil to slide. The positive pressure ($N=W\cos\alpha$) perpendicular to the slope produces frictional resistance to prevent the soil from sliding, which was called anti-slip force R . Therefore, the stability safety factor F_s of dryland slope was defined as follows^[25]:

$$F_s = \frac{R}{T} = \frac{W \cos \alpha \tan \varphi}{W \sin \alpha} = \frac{\tan \varphi}{\tan \alpha} \quad (3)$$

where, φ is the internal friction angle of the soil, ($^\circ$); α is the slope angle of the slope, ($^\circ$).

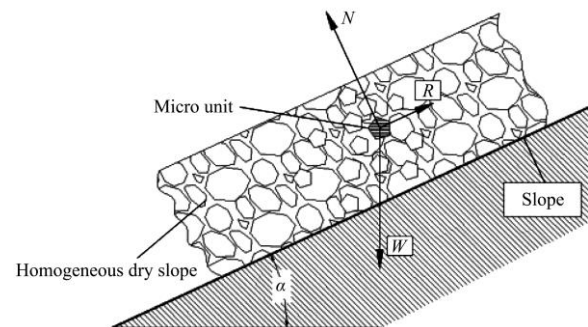


Figure 3 Schematic diagram of slope stability

The safety factor calculated according to Equation (3) had nothing to do with the weight and position of the micro-element, but only with the internal friction angle of the soil and the slope angle of the soil slope. When $F_s=1$, $\alpha=\varphi$, the slope angle, in this case, was called the natural resting angle^[26,27]. Slope stability was closely related to the natural resting angle of soil. When the slope angle was larger than the natural resting angle of soil, an unstable landslide would occur.

According to the structural characteristics of the ADP-SFR, too small a slope angle would cause the length of the frame to lengthen and increase the turning radius. On the contrary, too large a slope angle would lead to landslides, resulting in mixed soil samples. In order to obtain a suitable slope angle, the natural resting angle of soil was measured with soil fragmentation rate as a factor. The experimental material was soil after rotary tillage in Mengjin County, Henan Province, China. The soil moisture content was 15%-25%, and the internal friction angle was 25°-34°. In order to simulate different field conditions, the soil with different fragmentation rate was artificially proportioned. The angle between the cone pile formed by natural soil accumulation and the bottom surface was used to approximate the natural resting angle, and the average value was taken three times at each level, as shown in Table 2.

The results showed that the natural resting angle of field soil after rotary tillage was 37°-44°. The maximum slope angle of

shoveling or conveying soil was calculated based on the minimum natural resting angle. Due to the complicated forces on the soil slope on the ADP-SFR, the allowable safety factor of the slope should be appropriately improved by referring to GB 5033-2002 "engineering technical code for construction slope". The soil on the shovel was subject to the drag resistance along the horizontal direction, which prevents the soil from sliding, so the allowable safety factor here was 1.3; the soil on the conveyor belt was in a non-static state, so the allowable safety factor was 1.5. Combined with Equation (3), according to the allowable safety factor of the soil and the natural resting angle, the design inclination angles of the shovel and transport soil were determined to be 30.10° and 26.67° , respectively.

Table 2 Natural resting angle of field soil

No.	Soil fragmentation rate/%	Natural resting angle/(°)
1	40	42.87
2	50	43.11
3	60	40.56
4	70	38.90
5	80	35.54
6	90	37.31

3.2 Design of screening and weighing module

The distribution probability of soil particle size represents the relative content of each particle group in the soil. It is usually measured by the screening method. Since the solid particles in the agricultural soil after tillage were mostly coarse soil with strong permeability and no viscosity and plasticity, these characteristics indicate that the size grading of soil could be obtained by the screening method. Unlike engineering calculations, soil fragmentation rates in agriculture do not require drying operations. The traditional screening was to oscillate back and forth with a certain mesh aperture. Although this would lead to high labor intensity and low screening efficiency, it could reduce the disturbance to soil samples and control the measurement error within an acceptable range. When mechanical sampling was used, the collision of machine parts and samples might break many large soil masses, so it was necessary to design a reasonable screening and weighing equipment.

3.2.1 Design of screening module

The design of the screening module was the key to quickly obtain the size grading of soil. The reasonable structural design could not only realize fast sieve but also effectively reduce the damage to soil structure. For this purpose, a rotary circular screening module was designed, whose structure was shown in Figure 4a. The product of the screening module was shown in Figure 4b. Its overall structure includes diamond mesh, sprocket shaft and support frame, etc.

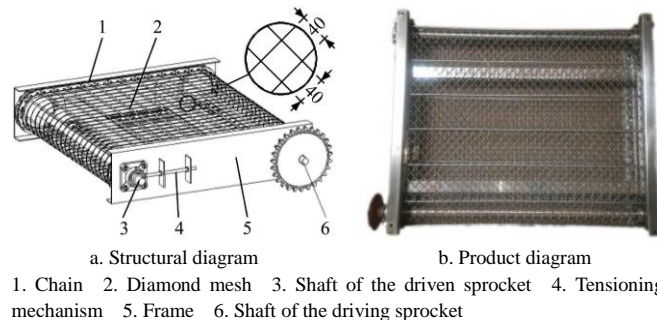


Figure 4 Rotary circulation screening module

During the screening process, the accumulation between fine

soil and coarse soil was easy to occur, which leads to the failure of fine soil to pass through the mesh, so the screening effect would become worse. Traditional artificial or mechanical vibrating sieves usually require shaking or vibrating sieves to cause the soil to flip on the screening surface, which increases the probability of fine particles passing through the screening, but also causes great damage to the coarse soil. According to the flow equation of solid particles, if the instantaneous velocity between solid particles was the same, the principle of rotary circular screening module was based on the following equation^[28]:

$$q = \frac{\Delta V \cdot \rho_s}{T} = 1000bhv_i \rho_s \quad (4)$$

where, q is the mass flow rate of solid particles, kg/s; ΔV is the volume of soil that passes through a certain cross-section, L; ρ_s is the density of solid particles, g/cm³; T is the time it takes a solid particle of volume b to pass through the section, s; b is the width of the cross-section formed by all particles, m; h is the height of the cross-section formed by all particles, m; v_i represents the instantaneous velocity of a solid particle, m/s.

According to Equation (4), if the mass flow of soil remains unchanged, that was, the soil mass entering the screening at any time was the same. When the width of the cross-section of soil remains unchanged, the height of the cross-section of soil (h) was inversely proportional to the instantaneous velocity (v_i). Therefore, the proportional reduction of the cross-sectional height of the soil was achieved by increasing the linear velocity of the mesh surface (screening velocity), so that the problem of accumulation between fine and coarse soil could be solved.

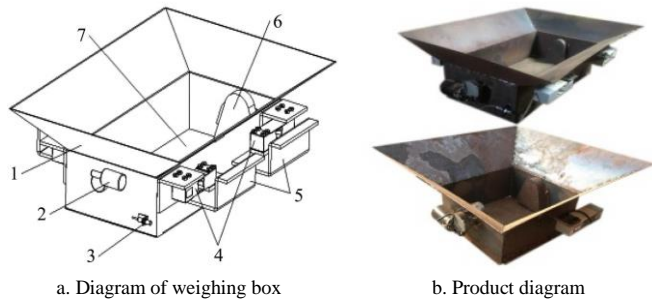
In order to evenly arrange the mesh holes on the screening mesh, a special mold was adopted to make the steel wire with a diameter of 2 mm into a diamond mesh according to certain rules. The material was made of 304# stainless steel to ensure that the mesh would not deform during the screening process. The two sides of the screening mesh were welded with the chain separately with a pitch of 38.1 mm. In order to prevent the overall deformation of the screening mesh from being too large, a series of shafts with a diameter of 10 mm were set every 150 mm. To prevent the soil from interfering with the mesh of the tooth chain, the middle section of the mesh was used to screening the soil. To reduce the length of the machine, the center distance of the rotary circulation screening mesh was 600 mm. The size of the holes in the mesh was determined as 40 mm according to the grading standard. The maximum swivel radius of the rotary circulation screening mesh was 70 mm, and the sprocket shaft drives the diamond mesh to rotate to realize the sieve movement of the soil.

3.2.2 Design of weighing box

The sifted soil was divided into two parts, one was fine soil with a diameter of less than 40 mm, and the other was large clods with a diameter of more than 40 mm. In order to obtain the weight information of the two parts of soil samples, a weighing box was designed, as shown in Figure 5a. Its structure was composed of a box, sensor, door structure and corresponding driving mechanism, which could complete the weighing and unloading of soil samples.

In general, the soil fragmentation rate after rotary tillage was more than 50%. The higher the fragmentation rate is, the larger the proportion of fine soil is. Therefore, the volume of the designed weighing box for broken soil was twice that of the weighing box for large clods. In order to ensure that soil samples do not overflow, when the maximum depth of soil sampling was 200 mm, the width of soil sampling was 500 mm, and the sampling

length was 500 mm, the volume of the weighing box for broken soil was designed to be 50 L, and the volume of the weighing box for large clods was designed to be 25 L. The products of the weighing module were shown in Figure 5b. The weighing box for broken soil was fixed with 4 sensors, and the weighing box for large clods was fixed with 2 sensors. The driving mode of the door structure was a capstan mechanism, through which the steel wire was pulled to make the door close, and the self-weight of the soil makes the door open. The drive motor adopts the decelerating motor with worm gear and worm, which had the self-locking function to ensure that the soil does not leak. To prevent the motor from overrunning, two sets of hall distance sensors were installed on the box body.



a. Diagram of weighing box
 1. Box body 2. Decelerating motor 3. Hall distance sensor 4. Strain type weighing sensor 5. Connection plate 6. Winch 7. Door structure

Figure 5 Structural diagram of weighing box

Due to the complicated field environment, when calculating the soil fragmentation rate, the detection platform may have a tilt angle with the horizontal plane, which would lead to a deviation between the sensor measurement data and the actual soil weight. In order to reduce the deviation, based on Equation (1), the weight module under a sampling interval calculates the soil fragmentation rate according to the following Equation:

$$E_{ij} = \frac{m_p}{m_p + m_q} \times 100 \quad (5)$$

$$m_p = \frac{\sum s_p}{\cos \theta_x \cos \theta_y} - M_{p0}, \quad p = 1, 2, 3, 4 \quad (6)$$

$$m_q = \frac{\sum s_q}{\cos \theta_x \cdot \cos \theta_y} - M_{q0}, \quad q = 1, 2 \quad (7)$$

where, m_p is the weight of the broken soil, kg; m_q is the weight of the large clods, kg; s_p represents the sensor measurement value of the weighing box for broken soil, kg; M_{p0} represents the no-load weight of the weighing box for broken soil, 15.17 kg; s_q represents the sensor measurement value of the weighing box for large clods, kg; M_{q0} represents the no-load weight of the weighing box for large clods, 11.58 kg; θ_x represents the inclination of the platform in the forward direction, ($^\circ$); θ_y represents the inclination of the platform along the axis, ($^\circ$).

By collecting the sensor measurement value and the change of inclination angle, the soil fragmentation rate was calculated. Without considering the sensor installation error, the precision of the weighing module designed in this study was no more than 12 g, which was far less than the maximum sample weight and could meet the measurement requirements.

In order to prevent soil samples from being mixed in two adjacent sampling intervals, the soil must be blocked from continuing to the screening module before reading the sensor signal. The weight threshold used to judge the end of sampling was called

the weighing cut-off threshold. Therefore, it was very important to select the weighing cut-off threshold, and the relationship between it and the sampling depth was as follows:

$$M_y = (1-k)BL\rho H \quad (8)$$

where, M_y is the weighing cut-off threshold, kg; k is the residual coefficient of soil sample on the screening module, and the value range is 0-1; B is the width of the sample, 0.5 m; L is the length of the sample, 0.5 m; ρ is the density of dryland soil after rotary tillage, g/cm³; H is the depth of the sample, mm.

Since the soil samples on the screening module had not been screened after blocking the transportation of soil samples, the residual coefficient of soil samples was set to modify the weighing cut-off threshold. According to the screening size in this study, the residual coefficient of the soil sample was 0.1. The value of the residual coefficient was related to the screening size of the screening module, the larger the screening size, the larger the value.

3.3 Design of control system module

3.3.1 Design of system hardware

The control system of the platform was composed of four parts: data processing center, motion control center, wireless control terminal and remote database of PC, as shown in Figure 6. The data processing center had the function of collecting signals and processing data. It could upload the detection data to the remote database of PC through the wireless data transmission station E32-TTL-100. The motion control center was used for the motion control of the detection process (belt motor, screening motor, movable bridge, door structure), which could receive the data from the data processing center, judge the weighing cut-off threshold and the state of the machine, and realize the continuous soil feeding, blocking and unloading of soil. The wireless control terminal communicates with the motion control center remotely through the wireless data transmission station E32-DTU(433L30), which could adjust the parameters and display the status of the whole machine, so as to help the operator quickly understand the status information of the whole machine.

3.3.2 Sensor and accessory parameters

The density of dryland soil after rotary tillage ranges from 1.6 to 2.2 g/cm³, and the maximum soil weight calculated according to the maximum sampling volume was less than 110 kg. Therefore, the strain type weighing sensor named LAB was selected. The range of a single sensor was 60 kg, the accuracy was 2 g, and the output signal was the analog signal. In order to realize the simultaneous detection of multiple sets of sensors, a digital-analog transmitter was used to integrate signals of each set of sensors (4 input signals and 2 output signals) and send them to the processing core. During the detection of soil fragmentation rate, the attitude information of the machine keeps changing. Therefore, the dynamic inclination sensor of model BWD-VG100 was selected, with dynamic accuracy of 2 $^\circ$ and static accuracy of 0.2 $^\circ$, which had high impact resistance. The accessory parameters of the ADP-SFR were shown in Table 3.

3.3.3 Design of system software

The system software of the ADP-SFR adopts C language for embedded development, and the processing core adopts STM32F103zet6. USART HMI software was used to modularized the wireless control terminal, and the display was TJC8048X570 capacitive touch screening. The visual interface was compiled as shown in Figure 7.

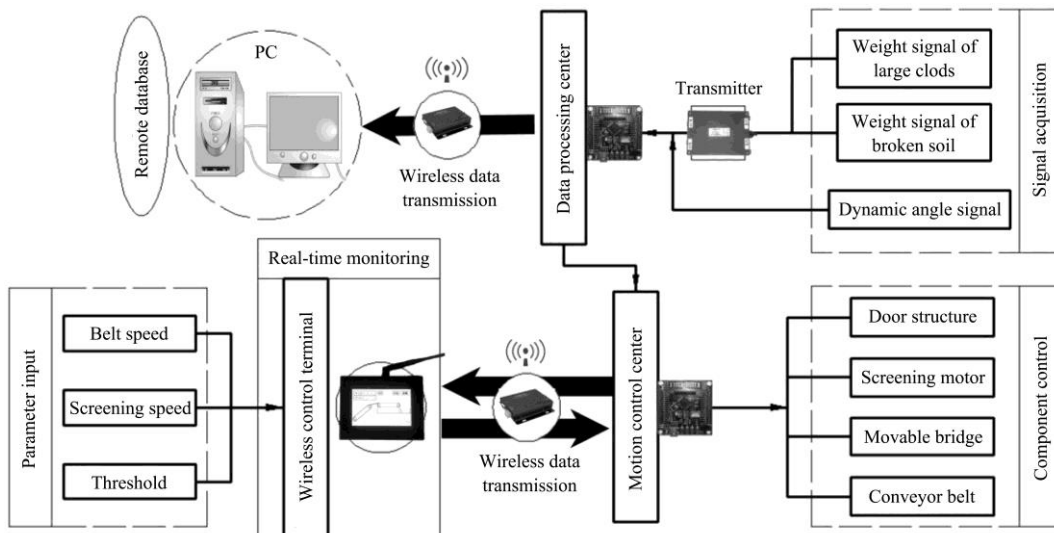


Figure 6 Automatic detection platform hardware system

Table 3 Accessories parameters of the platform

Name	Model	Number	Voltage	Measuring range	Precision
Strain type weighing sensor	LAE	6	5V DC	0-60 kg	2 g
Dynamic inclination sensor	BWD-VG100	1	5V DC	Longitudinal $\pm 90^\circ$, Transverse $\pm 180^\circ$	2°
Digital analog transmitter	ZNBSQ-Z	2	24V DC	—	—
Hall distance sensor	NJK-5001C	4	24V DC	0-10 mm	—

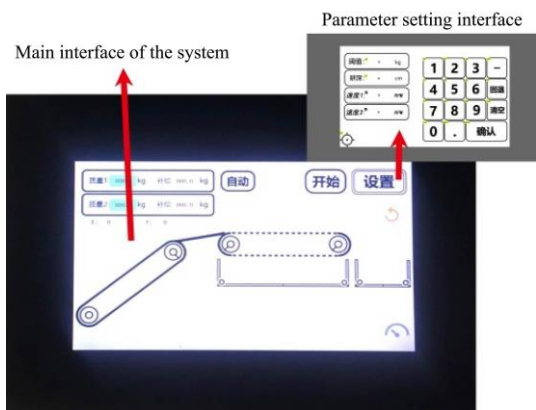


Figure 7 Visual interface

Firstly, the system initializes all sensor signals and sets detection parameters (sampling depth input, weighing cut-off threshold setting, measurement point number input); Then the system reset all the executing parts, and the reset state was belt motor and screening motor kept stopped, door structure kept normally closed, and movable bridge kept normally open; After the reset was completed, the conveying module was started first, the soil sample was continuously transported, and then the screening module was started; When the transportation of soil samples was stable, the movable bridge was closed through the timer so that the soil samples were transferred to the screening module; At the same time, the system continuously reads the attitude information of the detection platform and the weight information of the weighing module, which would be uploaded to the motion control center to decide whether the detection was finished or not; When the total mass of the soil sample in the weighing module reaches the pre-set threshold, the moving bridge was opened to block the subsequent soil sample; When all soil samples on the screening were fully entered into the weighing module, the soil fragmentation rate of a sampling interval was calculated according to the attitude information and weighing information. Such information would

also be stored in the remote database on PC; When the number of measuring points reaches the pre-set value, the detection of soil fragmentation rate of the trip was finished, and the system automatically carries out the detection of the next trip; When all three lines had been detected, the soil fragmentation rate was calculated by the system and uploaded to the PC terminal. The automatic detection process of the soil fragmentation rate was shown in Figure 8.

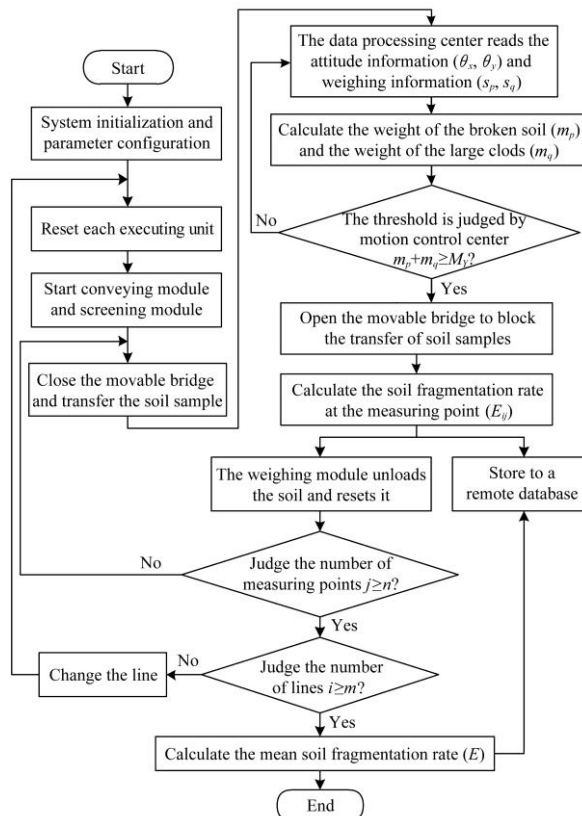


Figure 8 Automatic detection process for soil fragmentation rate

4 Experiments

4.1 Design of the screening module

4.1.1 Test materials and methods

The test material was taken from farmland in Mengjin County, Henan Province, where it was ploughed and then rotated. The type of test material was loam, the absolute moisture content was 15%-25%, the soil fragmentation rate was 60%-70%. In order to study the effect of screening speed on screening effect, screening speed was used as a factor for screening effect test. The indoor test site was shown in Figure 9.

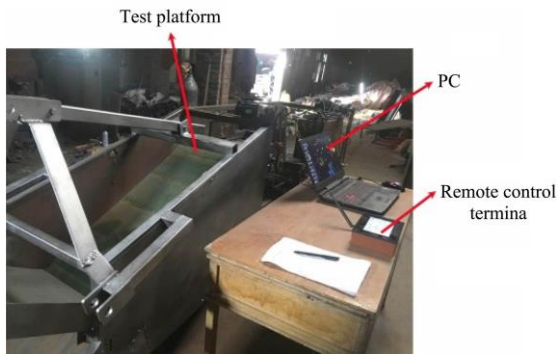


Figure 9 Indoor test site

The test soil was added into the feed tank, and the soil width was set as 500 mm and the soil thickness as 100 mm. During the screening test, keep the platform level and set the feed speed (forward speed of the tractor) to 0.14 m/s in advance. The horizontal component of the belt linear velocity should be greater than the forward velocity of the tractor to ensure that the soil does not accumulate. Therefore, the belt linear velocity was set at 0.2 m/s. According to the preliminary test, when the belt linear velocity exceeds about 1 m/s, the violent collision would occur when the soil enters the screening surface, which would seriously affect the screening effect. Therefore, the screening speed range was set to 0.2-0.8 m/s, within which 5 screening speed levels were set. According to Equation (8), the weighing threshold was set as 36 kg. When the screening was completed, the soil samples in the weighing module were respectively unloaded into different bins, and then manually selected and recorded the leakage rate and the error rate. Among them, lumps of less than 40 mm in the weighing box for large clods were used as the lumps of sieve leakage, and lumps of more than 40 mm in the weighing box for broken soil were used as the lumps of sieve error. The screening effect was reflected by the screening leakage rate and the screening error rate, and the relevant calculation formula was as follows:

$$e_l = \frac{m_l}{m_t} \times 100 \quad (9)$$

$$e_c = \frac{m_c}{m_t} \times 100 \quad (10)$$

where, e_l is the screening leakage rate, %; m_l is the weight of soil less than 40 mm in the weighing box for large clods, kg; m_t is the total weight of the soil sample, kg; e_c is the screening error rate, %; m_c is the weight of soil more than 40 mm in the weighing box for broken soil, kg.

4.1.2 Screening affect test results

In the screening test, the average value was obtained after repeated measurement for 5 times at the level of each screening speed, and the screening effect was shown in Figure 10.

In the test, it was found that the error screening rate of the ADP-SFR was no more than 1%, indicating that the screening

speed had little effect on the error screening rate. The triaxial dimensions of all the false-screening clods were counted, and it was found that their transverse dimensions were significantly different from their longitudinal dimensions (the longest side was more than 40 mm, while the other two sizes were both less than 2 cm), which may be an important reason for the incorrect screening. An amount of screening leakage occurred in the test, the maximum screening leakage rate was more than 13%. When the screening speed increases, the screening leakage rate decreases obviously. However, when the screening speed exceeded 0.5 m/s, the screening leakage rate showed an upward trend. The possible reasons for this situation were as follows: when the screening speed was close to the belt speed, with the increase of the screening speed, the clearance between clods gradually increases, and the possibility of the target clods passing through the sieve hole increases accordingly, which leads to the gradual reduction of the sieve leakage rate. As the screening speed continues to increase, some of the target clods were transported to the weighing box for large clods at the back before they had passed through the screening. When the screening line velocity was large, the kinetic energy obtained by the soil was also large, and some of the soil was mechanically damaged when it reaches the screening surface, which may also be the reason for the increase of the screening leakage rate. The test results show that when the screening speed was 0.5 m/s, the screening effect of the ADP-SFR was excellent, with the average screening leakage rate of 8.07% and the average screening error rate of 0.32%.

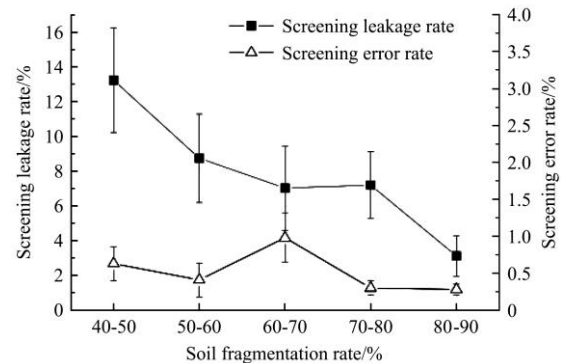


Figure 10 Test results of screening effect

4.2 Field performance test

4.2.1 Test method

In order to test the accuracy and reliability of the self-test platform for soil fragmentation rate, LX700 wheeled tractor was used as traction power to test the detection accuracy of soil fragmentation rate in the field quality test field of Mengjin County, Luoyang City in October 2019. The test site was shown in Figure 11. The temperature in the experimental field was 19 °C-21 °C and the soil moisture was 21%. In the experimental field, the foxtail millet had just been harvested and was ready to be spun for wheat.

Three pilot areas were selected for the experiment, with a total cultivated land area of about 0.3 hm². The 1GQNM-230 rotary cultivator (Henan Haofeng Agricultural Equipment Co., Ltd.) was used for rotary tillage in each pilot area. In order to obtain the test areas with different soil fragmentation rates, the operating parameters of rotary cultivator (forward speed, cutter shaft speed, rotary tillage depth) were set equally, and the three test areas were respectively subjected to one rotary tillage operation, two rotary tillage operations and three rotary tillage operations. The arrangement of measuring points in the test area is shown in Figure

12. According to the five-point measurement method, the soil fragmentation rate of each test area was manually detected and the detection time was recorded. In the test, the forward speed of the tractor was set to be about 0.5 km/h, the belt linear speed was set to 0.2 m/s, and the screening speed was set to 0.5 m/s. The soil sampling depth was determined according to the rotary tillage depth, and the soil sampling depth was set as 100 mm in this test. The multi-line and multi-point measurement method was adopted, and the field performance test was conducted according to 3 measuring points per stroke. The travel route was in the direction of the arrow in Figure 12. The test data of each trip was collected and the test time was recorded.



Rotation process Performance test process
Figure 11 Site of field performance test

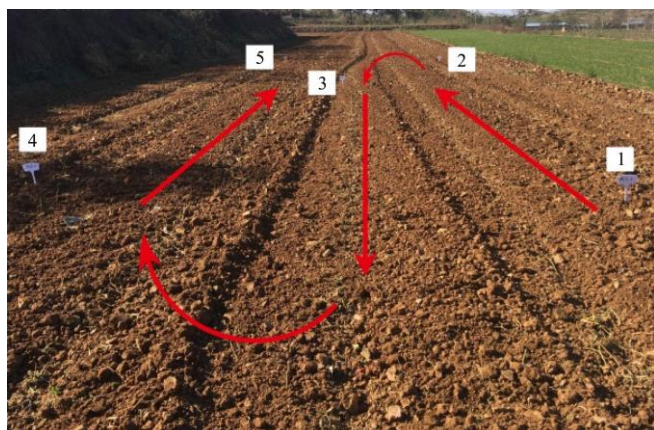


Figure 12 Arrangement of measuring points

4.2.2 Test results and analysis

The detection data of one of the test points as shown in Figure 13. The first part of the figure was the no-load stage, in which almost no soil enters the box. At this stage, the real-time soil fragmentation rate was in the stage of huge fluctuation, and the main influencing factors were the attitude change and vibration of the platform; The second part in the figure was the continuous screening stage, during which the soil was divided into crushed soil and large clods by the screening module, and the weight of the two boxes increases with the increase of soil volume. The real-time weight curve of broken soil was relatively gentle, while the real-time weight curve of large soil mass presents multiple burst signals. These shock signals were mainly generated by the oversized clods hitting the box, which would not affect the final detection results. As could be seen from the figure, when the weight of the soil reaches the weighing cut-off threshold (time 70 s), the soil was blocked, but the subsequent curve still shows a slow upward trend. This trend was due to the soil on the screening had not completely entered the box, increasing the total soil volume trend; The third part in the figure was the stabilization stage, during which the soil weight and real-time soil fragmentation rate curves were flat and straight, the data were relatively stable,

and almost no impact signal was generated.

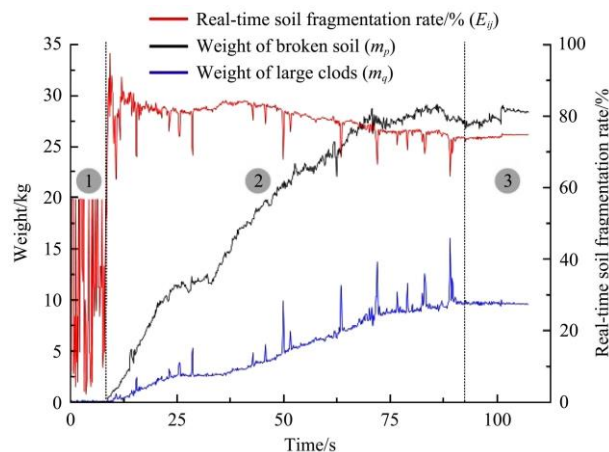


Figure 13 Real-time curve of soil fragmentation rate detection

Therefore, the data of stage No.3 was considered as the final result of this test. In this test, the soil fragmentation rate was finally stabilized at 74.72% and the root-mean-square error was less than 0.47%, so the mean value of the data in this section could be taken as the measurement value of the platform.

According to the test data of each measuring point, the test results of the ADP-SFR in the three test areas were calculated, and the results were compared with the results of the manual test, as shown in Table 4. After rotary tillage for different times, the soil fragmentation rates were 55.71%, 75.30% and 87.85%, respectively, indicating that soil fragmentation in different test areas was significantly different. Compared with the manual measurement, the test results of the corresponding soil fragmentation rate of this platform were 65.67%, 72.05% and 76.86%. In test area 3, the difference was the largest, but the maximum error was less than 11%; in test area 2, the difference was the smallest, with the error less than 4%. In this test, the threshold value of weighing was 36 kg, so the quality of the target soil sample was 40 kg, while the mean value of the actual soil total was 47.27 kg and the mean square deviation was 5.88 kg, indicating that the total amount of soil samples was stable each time. There were two reasons for the inconsistencies in the total amount of soil. First, there were shock signals in the detection process and error in the threshold determination in the dynamic detection process; Second, because of the heterogeneity of the soil in the field, the residual soil quality on the screening was different. In terms of the evaluation of detection efficiency, manual detection adopts two-person collaborative detection to complete the division of labor for soil collection and screening respectively, and the average manual detection time of each measuring point was more than 20 min. The maximum detection time of a single point of this platform was no more than 2 min, and the total detection time of each test area was no more than 30 min, which had obvious advantages over manual detection.

Due to the complexity of rotary tillage conditions, the spatial distribution of field soil was uncertain, so it was difficult to obtain the accurate soil fragmentation rate information of each measuring point. Therefore, the performance evaluation system adopted in this study was the human-machine interactive verification system, that was, the manual test was used as the benchmark for comparative verification. The purpose of this test was to verify the test performance of the ADP-SFR. The error of comparison with manual test could qualitatively indicate the actual test effect and applicability of this test method and system.

Table 4 Results of soil fragmentation rate detection

Test No.	Number of rotary tillage	Five-point method		Multi-line and multi-point method					Absolute error/%	
		Mean of soil fragmentation rate/%	Mean detection time/min	Total weight /kg	Soil fragmentation rate at the measuring point/%	Detection time at the measuring point/s	Soil fragmentation rate on the stroke/%	Mean of soil fragmentation rate/%		
1	1	55.71	23.54	39.40	67.58	97				+9.96
				43.75	72.62	79	67.43			
				48.90	62.10	68				
				43.93	69.25	49				
				48.69	52.10	61	64.97	65.67		
				41.78	73.57	79				
				45.67	68.80	77				
				40.64	56.72	88	64.60			
				43.21	68.29	79				
				40.52	85.06	72				
2	2	75.30	25.47	45.71	74.04	69	77.32		-3.25	
				48.52	72.85	93				
				56.61	68.69	67				
				55.49	72.80	70	74.18	72.05		
				49.56	72.95	73				
				45.34	76.34	64				
				68.32	51.47	67	67.35			
				42.78	74.23	69				
				47.38	70.72	69				
				43.14	81.48	64	76.60			
3	3	87.85	22.38	50.45	77.61	71			-10.99	
				46.40	71.10	71				
				45.03	84.92	79	77.54	76.86		
				47.09	76.61	71				
				49.83	76.44	67				
				52.86	78.14	68	76.43			
				45.17	74.72	69				

5 Conclusions

At present, manual operation is usually used to determine soil fragmentation rate. This method has a large workload and low efficiency, and cannot realize the fast processing of job data. Therefore, compared with manual detection, the detection method proposed in this study has obvious advantages in data acquisition speed and automation degree.

(1) In this study, aiming at the problem of difficult detection of soil fragmentation rate, an automatic detection platform for soil fragmentation rate is designed, which integrates the processes of soil sampling, soil screening, weighing and calculation of soil fragmentation rate. A multi-line and multi-point measurement method is proposed instead of the traditional five-point measurement method. The slide-slip problem of rotary tillage soil sampling is analyzed by using the non-viscous homogeneous dry slope model, the soil sample screening problem is solved by using the flow theory of fluid, and the weighing problem of soil sample after sieving is solved by using multi-sensor fusion.

(2) An automatic soil fragmentation rate detection system composed of a data processing center, motion control center, wireless control terminal and PC remote database was designed. C language was adopted for embedded development, and USART HMI software was used for the modularized design of wireless control terminal, which realized remote control and data acquisition of the platform and provided data support for evaluation of rotary

tillage operation effect and sowing in agricultural production.

(3) Mechanized sampling increases the rate of soil breakage. Generally speaking, the smaller the size of the clod, the stronger the crushing effect of the shovel. According to China's agricultural machinery industry standards, when analyzing the soil fragmentation rate of agricultural machinery, the target soil block diameter should not be less than 40 mm. For a block of this size, the spade is hardly damaged. Therefore, this work believes that the use of mechanized sampling will have an impact on the rate of soil breakage, but the impact is acceptable.

(4) The screening effect test shows that when the screening speed is 0.5 m/s, the screening effect of this platform is excellent, with an average screening leakage rate of 8.07% and an average screening error rate of 0.32%. In October 2019, the field performance test of the automatic detection platform for soil fragmentation rate was carried out in Mengjin County, Luoyang City. Compared with the results of manual measurement, the maximum detection error is less than 11%, and the minimum detection error is less than 4%. The maximum detection time of a single point is not more than 2 min, and the total detection time of each test area is not more than 30 min, which has obvious advantages over manual detection.

The future research work is to research the influencing factors of soil fragmentation rate. The relationship between working resistance, soil moisture content, organic matter content and soil fragmentation rate would determine by statistical analysis. On the

basis of these researches, the soil fragmentation detection equipment could be integrated into the rotary tiller to realize the online detection of the effect of rotary tillage.

Acknowledgements

This work was supported by the National Key R&D Program of China (Grant No. 2017YFD0700300), Key Research and Development Program of Yunnan Province (Grant No. 2018ZC001-3) and Intelligent Manufacturing & standardization of the Ministry of Industry and Information Technology of the People's Republic China (No. 2018GXZ1101011).

[References]

- [1] Zhao J G, Wang A, Ma Y J, Li J C, Hao J J, Nie Q L, et al. Design and test of soil preparation machine combined subsoiling rotary tillage and soil breaking. *Transactions of the CSAE*, 2019; 35(8): 46–54. (in Chinese)
- [2] Zhang C L, Xia J F, Zhang J M, Zhou H, Zhu Y H, Wang J W. Design and experiment of knife roller for six-head spiral straw returning cultivator. *Transactions of the CSAM*, 2019; 50(3): 25–34. (in Chinese)
- [3] Zhao S H, Wang J Y, Yang C, Chen J Q, Yang Y Q. Design and experiment of stubble chopper under conservation tillage. *Transactions of the CSAM*, 2019; 50(9): 57–68. (in Chinese)
- [4] Xu X C, Chen S X, Jiang L F. On compaction characteristics and particle breakage of soil-aggregate mixture. *Advances in Intelligent Systems Research*, 2015; 126: 83–87.
- [5] Yudina A V, Fomin D S, Kotelnikova A D, Milanovskii E Y. From the notion of elementary soil particle to the particle-size and microaggregate-size distribution analyses: A review. *Eurasian Soil Science*, 2018; 51(11): 1326–1347.
- [6] Hu F N, Liu J F, Xu C Y, Wang Z L, Liu G, Li H, et al. Soil internal forces initiate aggregate breakdown and splash erosion. *Geoderma*, 2018; 320: 43–51.
- [7] Hu F, Li S, Xu C, Gao X, Miao S, Ding W, et al. Effect of soil particle interaction forces in a clay-rich soil on aggregate breakdown and particle aggregation. *European Journal of Soil Science*, 2019; 70(2): 268–277.
- [8] Feng D L, Fang Y G. Theoretical and experimental study on multi-scale mechanical properties of soil. *Soil Mechanics and Foundation Engineering*, 2015; 52(4): 189–197.
- [9] Zheng K, McHugh A D, Li H W, Wang Q J, Lu C Y, Hu H N, et al. Design and experiment of anti-vibrating and anti-wrapping rotary components for subsoiler cum rotary tiller. *Int J Agric & Biol Eng*, 2019; 12(4): 47–55.
- [10] Bayat H, Zadeh G E. Estimation of the soil water retention curve using penetration resistance curve models. *Computers and Electronics in Agriculture*, 2018; 144: 329–343.
- [11] Goodin C, Priddy J D. Comparison of SPH simulations and cone index tests for cohesive soils. *Journal of Terramechanics*, 2016; 66: 49–57.
- [12] Celik A, Raper R L. Comparison of various coulter-type ground-driven rotary subsoilers in terms of energy consumption and soil disruption. *Soil Use and Management*, 2016; 32(2): 250–259.
- [13] Wang J W, Zhang C L, Xu C L, Wang J F, Kong Y J, Zhao J L. Parameters optimization on flattening component of combined cultivating implement. *Transactions of the CSAM*, 2013; 44(2): 34–37, 11. (in Chinese)
- [14] Qin K, Ding W M, Fang Z C, Du T T, Zhao S Q, Wang Z. Design and experiment of plowing and rotary tillage combined machine. *Transactions of the CSAE*, 2016; 32(16): 7–16. (in Chinese)
- [15] Hao J J, Yu H J, Zhao J G, Li J C, Ma Z K, Cai J J. Design and test of wedge drag reduction rotary blade. *Transactions of the CSAE*, 2019; 35(8): 55–64. (in Chinese)
- [16] Zhou H, Zhang J M, Xia J F, Tahir H M, Zhu Y H, Zhang C L. Effects of subsoiling on working quality and total power consumption of high stubble straw returning machine. *Int J Agric & Biol Eng*, 2019; 12(4): 56–62.
- [17] Li Y W, Zhang G Y, Zhang Z, Zhang Y, Hu T D, Cao Q Q. Development of low power-consumption multi-helical rotavator for small vertical-shaft deep-cultivator. *Transactions of the CSAE*, 2019; 35(4): 72–80. (in Chinese)
- [18] Du X W, Yang X L, Pang J, Ji J T, Jin X, Chen L. Design and Test of Tillage Depth Monitoring System for Suspended Rotary Tiller. *Transactions of the CSAM*, 2019; 50(8): 43–51. (in Chinese)
- [19] Wang J W, Yang W P, Sun X B, Li X, Tang H. Design and experiment of spray and rotary tillage combined disinfection machine for soil. *Int J Agric & Biol Eng*, 2019; 12(1): 52–58.
- [20] Jin X, Li D Y, Ma H, Ji J T, Zhao K X, Pang J. Development of single row automatic transplanting device for potted vegetable seedlings. *Int J Agric & Biol Eng*, 2018; 11(3): 67–75.
- [21] Liu J L, Zhang L L, Fu Q, Ren G Q, Liu L, Yu P, et al. Spatial variability of soil particle-size distribution heterogeneity in farmland. *Transactions of the ASABE*, 2018; 61(2): 591–601.
- [22] Liu Y, Zhao B B, Yin K L, Chen L X, Gui L, Liang X. Sensitivity analysis of maliulin landslide stability based on orthogonal design. *Earth Science*, 2019; 44(2): 677–684. (in Chinese)
- [23] Yu K Y, Yao X, Qiu Q R, Liu J. Landslide spatial prediction based on random forest model. *Transactions of the CSAM*, 2016; 47(10): 338–345. (in Chinese)
- [24] Wang Z Y, Cao J J, Lin Z X, Wu Z Q. Characteristics of soil particles in the Xiaohulishan deposit, Inner Mongolia, China. *Journal of Geochemical Exploration*, 2016; 169: 30–42.
- [25] Duan Z H, Qiu W, Ding W M, Liu Y D, Ouyang Y P, et al. Tilting stability analysis and experiment of the 3-DOF lifting platform for hilly orchards. *Int J Agric & Biol Eng*, 2018; 11(6): 73–80.
- [26] Bu X H, Fu R H, Li J D, Huang Y. Internal factors of the failure of granular mixtures slope. *Journal of Yangtze River Scientific Research Institute*, 2016; 33(9): 116–120. (in Chinese)
- [27] Song Y S, Xu X, Yang S, Gao M. Influence of water content on shear strength of granite residual soil in Huangdao area. *Journal of Shandong University of Science and Technology (Natural Science)*, 2019; 38(4): 33–40. (in Chinese)
- [28] Ding Y Q, Ding W M. Theoretic analysis and design of a new mass flow rate measurement method for solid granule material. *Journal of Electronic Measurement and Instrumentation*, 2007; 21(6): 45–48. (in Chinese)